Two-dimensional dynamical model for step bunching and pattern formation induced by surface reconstruction

Hyeong-Chai Jeong and John D. Weeks
Institute for Physical Science and Technology, University of Maryland, College Park, Maryland 20742
(Received 19 September 1997)

Surface reconstruction on sufficiently wide terraces on a vicinal surface can cause the formation of step bunches. We consider this process in the nucleation regime using a two-dimensional (2D) dynamical model that describes both surface reconstruction and the effects of the growth of a reconstructed facet on the motion of neighboring steps. When there is local mass transport, we show that the growth of a reconstructed facet can induce the growth of a similar facet nearby, leading to regular arrangements of flat facets separated by step bunches and to other characteristic 2D step patterns. [S0163-1829(98)02108-0]

I. INTRODUCTION

Surface reconstruction can often cause a vicinal surface with a single macroscopic orientation to rearrange or facet[1] into ''flat'' reconstructed terraces and much more sharply inclined unreconstructed regions with closely bunched steps.[2–6] In this paper, we study the dynamics of this faceting and the resulting step patterns that form using a two-dimensional (2D) model that describes the coupling of the reconstruction process to the motion of individual steps. This generalizes our previous work, which considered a 1D step model[7] and treated the reconstruction in a less general way.[8]

In most cases the reconstruction occurs on a particular low-index ''flat'' face, and lowers its free energy relative to that of an unreconstructed surface with the same orientation. However, the same reconstruction that produces the lower free energy for the flat face generally *increases* the energy of surface distortions such as steps that disturb the reconstruction. Thus on vicinal surfaces reconstruction is often favored only on terraces wider than some *critical terrace width* w_c. When steps are initially distributed with average step space w_a much smaller than the critical width w_c, step fluctuations leading to the formation of a sufficiently wide terrace — a ''critical nucleus'' — are required for the reconstruction to begin. Continued growth of the reconstruction will make the vicinal surface facet into distinct regions consisting of reconstructed terraces and closely bunched steps.

In agreement with this picture, experiments on several systems including the 7×7 reconstruction on the Si(111) surface[2] and the formation of $(n\times1)$ oxygen chains on the O/Ag(110) surface[4] show reconstruction only on sufficiently wide terraces. However, faceting experiments on these and some other systems such as GaAs(100), Pt(111), and Au(111), show a noticeable regularity in the size and spacing of the flat facets[2,3,5,6] though the extent of regularity is different depending on the system. These regularities seem hard to reconcile with a picture of random nucleation of the faceted regions. While a number of different factors can contribute to the facet spacing in particular experiments, we show here that there exists a rather general *kinetic* mechanism that can lead to regular features in the faceting process.

In the following section, we introduce an effective 2D Hamiltonian that describes the energetics of individual step configurations and the effects of reconstruction on the terraces. The dynamical equations for step motion and reconstruction are then given in terms of a step chemical potential and an effective local reconstruction field as determined from the effective Hamiltonian. These equations of motions can be numerically integrated; the results are presented in Sec. III. We first study the lateral and normal growth rate of an isolated nucleated facet. Then we show how an *induced nucleation mechanism*[7,8] can produce a regular array of step bunches in the faceted surface and other 2D patterns. It is also shown here that when thermal fluctuations are taken into account the induced nucleation mechanism leading to regular features in the faceted surface can occur under even more general conditions than what the previously studied deterministic models[7,8] would predict.

II. MESOSCOPIC MODEL

Several different representations of a given surface are possible depending on the scale at which the surface is investigated.[9] On a *microscopic scale*, one can try to specify the surface by focusing on the positions of individual atoms and study the evolution of morphology from the motions of individual atoms on the surface.[10] In practice, this is possible only numerically and is usually limited to very small systems and for very short times. Hence, in most microscopic studies, one considers a model Hamiltonian that simplifies the possible configurations and the interactions of atoms at the surface and that incorporates only the most relevant excitations for the morphology changes under consideration. This approach usually leads to *discrete* descriptions of the surface as illustrated in Fig. 1(a), which shows a typical surface configuration of a terrace-step-kink model along with a critical width model[7,8] for reconstruction. In the critical width model, terraces with width wider than some w_c (represented by the shaded area) are assumed to be reconstructed.

On a *coarse-grained continuum scale*, the surface configurations are specified by smooth variables that are obtained by integrating out or averaging over short-wavelength fluctuations at the atomic scale. For example, Fig. 1(c) illustrates a surface represented by *continuous* surface height variables, $z(x,y)$, and a continuous reconstruction field,

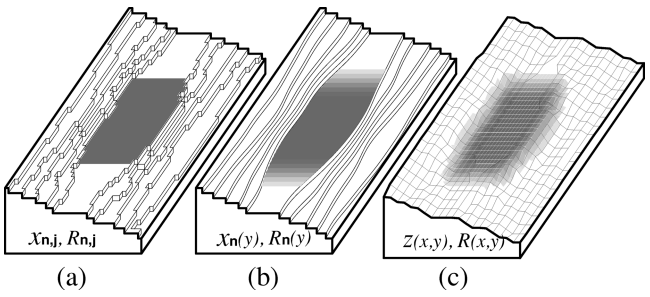

FIG. 1. Schematic surface configurations on different scales. (a) A typical step configuration in the terrace-step-kink model with a reconstructed facet nucleus when reconstruction occurs on all the terraces (shaded area) wider than w_c. The surface and reconstruction profiles are specified by discrete variables, $x_{n,j}$ and $R_{n,j}$. (b) By coarse graining along the nominal step direction, we get continuum step and reconstruction configurations described by $x_n(y)$ and $R_n(y)$. However, the surface height still takes on discrete values and the reconstruction profile changes discretely between neighboring terraces. (c) The surface is described by a continuous height variable, $z(x,y)$ if it is coarse grained over several terraces including steps. The small squares indicate grid lines. The reconstruction profile $R(x,y)$ is continuous over the surface.

$R(x,y)$, obtained by averaging the results of a discrete model using some appropriately chosen ''smearing kernel.'' Here $z(x,y)=\Sigma_k K_{xy}(x-x_k,y-y_k)h_k$, and $R(x,y)=\Sigma_k K_{xy}(x-x_k,y-y_k)R_k$, with a smearing kernel $K_{xy}(|\vec{r}|)\sim e^{-|\vec{r}|}$, where h_k is the height of the kth column at (x_k,y_k) in Fig. 1(a) and $R_k=1$ ($R_k=0$) if the kth column is reconstructed (unreconstructed). The physical properties of these coarse-grained surfaces are investigated (often analytically) in a continuum approach using a phenomenological Hamiltonian (free-energy functional) of the Landau-Ginzburg type.[11] This approach is known to describe well the long-wavelength properties of the surfaces in many cases, especially *above* the roughening transition temperature T_R.[12]

However, continuous height variables may not yield the best description for the surface below T_R. One loses the information about properties of individual steps, which are some of the main features of the surface at low temperature. Furthermore, a reconstructed region is expected to have a sharp boundary near the step if reconstruction happens only on sufficiently wide terraces. Thus it is difficult to represent the reconstruction properly using an isotropic coarse graining like that illustrated in Fig. 1(c). On these surfaces, it seems better to focus on the properties of *individual steps and their interactions*. Figure 1(b) illustrates a surface configuration in a *mesoscopic* approach where individual steps are identified with a discrete step index n, but the behavior of each step is investigated from a continuum approach. A continuum description of the step positions can be obtained by averaging over short-wavelength fluctuations such as kinks in the step configurations. For example, the continuum step position $x_n(y)$ shown in Fig. 1(b) is obtained by $x_n(y)=\Sigma_j x_{n,j}K_y(y-y_j)$, with a smearing kernel $K_y(r)\sim e^{-|r|}$ where $x_{n,j}$ is the discrete step position in Fig. 1(a) and y_j is the y coordinate of the jth segment.

A continuous description of terrace reconstruction, described by $R_n(y)$, is obtained in a similar manner. The kinetics of the reconstruction is believed to be much faster than the kinetics of the step rearrangements.[13] Once reconstruction happens on some part of a terrace, the expansion of the reconstructed region in a terrace to the full terrace width is thought to happen much faster than the step movement to further expand the terrace width in the y direction. When we describe the reconstruction dynamics on the time scale of the movement of a typical step segment, it thus seems reasonable to consider a (whole) terrace segment as the unit of reconstruction or deconstruction. Therefore, in a discrete description of reconstruction we can assign discrete value, $R_{n,j}=1$ or 0 to the jth segment of the nth terrace depending on whether it is reconstructed or not. The continuous variable $R_n(y)$ representing reconstruction on the nth terrace in the mesoscopic model is then given by $R_n(y)=\Sigma_j R_{n,j}K(y-y_j)$ just as for the step positions.

A. Effective Hamiltonian

To describe the evolution of surface morphology and reconstruction in terms of these continuum variables, $\{x_n(y)\}$ and $\{R_n(y)\}$, we need to provide an effective Hamiltonian for arbitrary configurations of these coarse-grained variables. We can think of at least two formal ways of obtaining the effective Hamiltonian from microscopic models. First, we can imagine summing over all microscopic configurations consistent with a given coarse-grained step and reconstruction configuration, $\{X_n(y)\}=(\{x_n(y)\},\{R_n(y)\})$. As in real-space renormalization-group calculations,[14] we could get an effective Hamiltonian in principle by calculating the logarithm of the partial sum of Boltzmann factors:

$$-H(\{X_n(y)\})/k_BT\equiv\ln\left[\sum_{\{X^m_{n,j}\}\in\{X_n(y)\}}\exp\left(-\frac{H^m(\{X^m_{n,j}\})}{k_BT}\right)\right], \tag{1}$$

where $\{X^m_{n,j}\}=(\{x^m_{n,j}\},\{R^m_{n,j}\})$ is a configuration in the microscopic model with Hamiltonian H^m.

Alternatively, in analogy with density-functional methods for inhomogeneous fluids,[15] we can consider auxiliary external fields $\{\phi_x(x,y)\}$ and $\{\phi_R(x,y)\}$ that couple linearly to the step positions and reconstructed regions such that a given arbitrary configuration of $\{x_n(y)\}$ with $\{R_n(y)\}$ will be the equilibrium state. The free energy of this system, calculated by taking the trace over all configurations in the presence of the external fields, will be a functional of $\{\phi_x(x,y)\}$ and $\{\phi_R(x,y)\}$, and includes the direct linear contribution from the external fields. If we subtract these linear terms in the field we get the ''intrinsic'' free energy of the nonuniform system, which we use as our effective Hamiltonian. Technically, this generates a Legendre transform giving the free energy as a functional of the configurations $\{x_n(y)\}$ and $\{R_n(y)\}$ rather than the auxiliary fields.

In practice, both formal methods are not easy to carry out for general step configurations, though the second method has been successfully applied to calculate the edge energy of nonuniform, quasi-1D configurations.[16] Here we will not consider such formal development further. Rather, we introduce a mesoscopic model Hamiltonian that incorporates the known results for two simpler systems, a 1D fluctuating interface[17,18] and a 2D array of fluctuating steps with uniform

average spacing,[19,20] and use heuristic arguments to describe the contribution from reconstruction:

$$H=\sum_n \int dy\left[V(w_n(y),R_n(y))+\frac{\tilde{\beta}}{2}(\partial_y x_n)^2 + \frac{D_r}{2}w_n(y)(\partial_y R_n)^2\right]. \quad (2)$$

Here $w_n(y)\equiv x_{n+1}(y)-x_n(y)$ is the local terrace width of the nth terrace at position y, $\tilde{\beta}$ is the line tension that controls the extent of fluctuation of an *isolated* step, and the sum is over all steps (other symbols are defined below).

In our previous studies[7,8,21] of reconstruction-driven faceting, we used an even simpler model Hamiltonian without an explicit reconstruction field. This was defined in terms of step configurations only through the assumption that every terrace segment with width wider than the critical width w_c is reconstructed. Clearly, this minimal model for reconstruction does not take proper account of the interface energy associated with a *domain boundary* between reconstructed and unreconstructed regions on the same terrace. However, in the earlier work we focused on the growth of a previously formed reconstructed nucleus where the interface energy remains essentially constant and hence does not affect the dynamics.

In this paper we consider the more general case and take account of both the interfacial energy and the reconstruction profile explicitly. In particular, the third term of the Hamiltonian of Eq. (2), $\frac{1}{2}D_r w_n(y)[\partial_y R_n(y)]^2$ represents the interface energy between reconstructed and unreconstructed regions on the nth terrace. This term makes the initial formation of an isolated reconstructed nucleus more difficult than the growth of reconstruction on a local terrace adjacent (in the y direction) to an already reconstructed region.

The first term, $V(w_n(y),R_n(y))$ describes the effective step-step interactions between the nth step and the $(n+1)$th step where $R_n(y)$ represents the ''fractional coverage of reconstruction'' on the terrace between them. As in the previous studies,[7,21] we assume that the appropriate form of this step-step interaction can be obtained from a 1D (projected) free-energy density with the slope $s=1/w$ equal to the local width. The standard form[19,20] (for *unreconstructed* vicinal surfaces) is given by $f_u(s)=f^0+\beta s+gs^3$, where f^0 is the surface free-energy density of the reference plane, β is the free-energy cost per unit length for creating an isolated step, and gs^3 is the free energy due to step-step interactions.[22] For the surface with uniform reconstruction coverage R, with $0\leq R\leq 1$, we assume that the 1D free-energy density still has the same functional form,

$$f(s,R)=f^0(R)+\beta(R)s+g(R)s^3, \quad (3)$$

but with R-dependent coefficients.

The experimental fact that reconstruction occurs only on sufficiently wide terraces can be understood within a model with straight steps by assuming that the free energy of the reconstructed flat surface has a lower energy ($-\epsilon_R$ per unit area) than the unreconstructed one but effectively a higher energy cost (ϵ_s per unit length) for forming an isolated step.[23] The free energy of the fully reconstructed surface, $f(s,R=1)=(f^0-\epsilon_R)+(\beta+\epsilon_s)+gs^3$, is lower than that of the unreconstructed surface, $f(s,R=0)\equiv f_u(s)$ when the slope s is less than $s_c\equiv\epsilon_r/\epsilon_s$. With a proper smoothing scheme, the effect of reconstruction is expected to be proportional to R; hence, we use $f^0(R)=f^0-\epsilon_R R$ and $\beta(R)=\beta+\epsilon_s R$ in the continuum approach.[24] We now follow our previous arguments[7,8] and approximate the interaction term $V(w,R)$ in the 2D model Hamiltonian in Eq. (2) by the interaction $f(1/w,R)w$ of a 1D model at the *local* width w:

$$V(w,R)=(f^0-\epsilon_R R)w+(\beta+\epsilon_s R)+g/w^2. \quad (4)$$

This local approximation ignores smaller edge energy terms.[16] These can be important in some cases, but no major error will arise in the applications considered here.

This completes the description of the effective Hamiltonian in Eq. (2), which determines the equilibrium properties of our model. We now define the terms that will control the step and reconstruction dynamics.

B. Step chemical potential and local reconstruction field

In a step approach, surface motion results from adsorption or emission of atoms at the step edge. Adatom attachment or detachment at a step corresponds to a small variation of the continuous step position. Therefore, the free-energy change due to an atom attachment on the step is proportional to the functional derivative with respect to the step position field, $x_n(y)$, of the effective step Hamiltonian of Eq. (2). We define the *step edge chemical potential*,[25] $\mu_n(y)$, as the change in the free energy when we add an atom to the nth step at position y. If Ω is the area occupied by an atom, $\mu_n(y)$ is given by

$$\mu_n(y)\equiv-\Omega\frac{\delta H}{\delta x_n(y)} \approx\Omega[\partial_w V(w,R)|_{\substack{w_n(y)\\R_n(y)}}-\partial_w V(w,R)|_{\substack{w_{n-1}(y)\\R_{n-1}(y)}}]+\tilde{\beta}\Omega\partial_y^2 x_n. \quad (5)$$

For simplicity, we have ignored the functional derivative of the third term in Eq. (2), which is of the same order as the previously ignored R dependence of $\tilde{\beta}$. However, no new problems arise if both effects are taken into account, and they may be important in some applications.

The term $\partial_w V(w,R)|_{w_n(y),R_n(y)}$ in Eq. (5) has dimensions of force per unit length and can be interpreted as an effective *pressure* on the step associated with terrace n. Thus $\mu_n(y)$ depends on the local (linearized) curvature $\partial_y^2 x_n$ of the step and on the difference in pressure from terraces behind and in front of the step. For the step interactions of Eq. (4), the effective pressure on the step has two sources: reconstruction ($\epsilon_R R$), and step repulsions ($2g/w^3$). Thus the step chemical potential is written as

$$\mu_n(y)=-\Omega\{\epsilon_R[R_{n-1}(y)-R_n(y)] +2g[w_{n-1}^{-3}(y)-w_n^{-3}(y)]+\tilde{\beta}\partial_y^2 x_n(y)\}. \quad (6)$$

To describe the dynamics of reconstruction, we define a *local reconstruction field* $B_n(y)$ that couples linearly to the reconstruction coverage at position y, given by $w_n(y)R_n(y)$. Formally this is defined by

$$B_n(y) \equiv -\frac{1}{w_n(y)} \frac{\delta H}{\delta R_n(y)}. \tag{7}$$

For the effective Hamiltonian of Eq. (2), we have

$$B_n(y) = \epsilon_R - \epsilon_s / w_n(y) + D_r \partial_y^2 R_n(y). \tag{8}$$

If the terrace size goes to infinity ($w_n \to \infty$) and R_n is uniform in a terrace ($\partial_y^2 R_n = 0$), $B_n(y)$ takes on the constant value of ϵ_R as expected. In a finite width terrace, there are boundary effects from the steps. Since a step on a reconstructed surface costs more energy, ϵ_s per unit length, than on an unreconstructed one, steps at the boundary of a terrace provide an effective field, with average value $\epsilon_s / w_n(y)$, opposing the reconstruction.

The third term, $D_r \partial_y^2 R_n$, in Eq. (8) tends to make reconstruction uniform in a terrace to reduce the interface energy in the y direction. The magnitude of the interface energy is parametrized by D_r. When D_r tends to zero (small interface energy), local terraces with widths $w(y)$ larger than $w_c \equiv \epsilon_s / \epsilon_R$ have a net positive field for the reconstruction [$\epsilon_R > \epsilon_s / w_n(y)$]. Hence a terrace with local width $w(y) > w_c$ will increase its reconstruction coverage regardless of the coverage of the neighboring regions in the y direction. This reduces to the previously studied model for reconstruction.[7] However, for large D_r, the nucleation of reconstruction at a local terrace region with width around w_c is unlikely unless a sufficiently long lateral region of width w_c or wider is formed. In contrast, a local terrace with width w_c *adjacent* (in y direction) to an already reconstructed region will be more easily reconstructed. In this sense, w_c is the ''critical width for lateral growth'' in the y direction[8] and is in general smaller than the critical width for the initial nucleation of reconstruction for the model with non-zero D_r.

C. Models for reconstruction and step dynamics

To model the dynamics of reconstruction and step motion, we make a linear kinetics approximation, assuming that the rates of change of perturbations in the reconstruction and step position fields are proportional to the associated change in free energy as calculated from the effective Hamiltonian in Eq. (2). The kinetic equation for the reconstruction is easy to write down since the extent of reconstruction is not a conserved quantity. We simply assume that the reconstruction rate is proportional to the local reconstruction field:

$$\begin{aligned} \partial_t R_n(y) &= \Gamma_R B_n(y), \\ &= \Gamma_R [\epsilon_R - \epsilon_s / w_n(y) + D_r \partial_y^2 R_n(y)], \end{aligned} \tag{9}$$

where Γ_R is the inverse of the ''friction'' coefficient relating the ''velocity'' $\partial_t R$ to the ''force'' B.

However, since the step motion results from the movement of atoms at steps, the kinetics of step motion depends on the mechanism of mass transport on the surface. Before considering general fluctuating 2D step arrays, let us consider a quasi-1D array of straight steps. There are two limiting cases of mass transport depending on whether the atom exchange is limited to neighboring steps (*local movement*) or not (*global movement*). Mass movement is *global* if atoms at a step edge are exchanged with a vapor reservoir (evaporation-condensation) or with a terrace reservoir that forms by fast direct adatom hops between different terraces. In the latter case, steps move according to the chemical potential difference between the step and the reservoir:

$$\partial_t x_n = \frac{\Gamma_A}{\Omega k_B T} [\mu_n - \mu_{\mathrm{res}}], \tag{10}$$

where Γ_A is the mobility of the step edge as defined by Bartelt *et al.*[26] It is given as $\Gamma_A = \Gamma_+ + \Gamma_-$ where Γ_+ (Γ_-) is the mobility of the step edge from mass exchange with the upper (lower) terrace when the global reservoir is formed on terraces.

When the mass movement is *local*, as in mass movement through surface diffusion without direct adatom hops between terraces, the motion of neighboring steps is strongly coupled together. The step velocity is then assumed to be controlled by the chemical potential difference between the step and its nearest neighbors:

$$\partial_t x_n = \frac{\Gamma_e(w_n)}{\Omega k_B T} [\mu_n - \mu_{n+1}] + \frac{\Gamma_e(w_{n-1})}{\Omega k_B T} [\mu_n - \mu_{n-1}]. \tag{11}$$

Here $\Gamma_e(w)$ is some effective adatom exchange coefficient between neighboring steps, which in general depends on the distance between the steps.[27] In the quasistatic approximation, one can obtain $\Gamma_e(w)$ by considering the diffusion equation on the terrace under the boundary conditions at step n arising from the mass conservation.[28] As shown in the Appendix, this result can be also obtained intuitively by considering an analogy with the conductivity in a series electric circuit, and we find

$$\Gamma_e(w) = \left[\frac{1}{\Gamma_+} + \frac{w}{D_s c_0 \Omega^2} + \frac{1}{\Gamma_-} \right]^{-1}, \tag{12}$$

where D_s is the surface diffusion constant and c_0 is the equilibrium adatom density on the terrace far from the step at which the terrace chemical potential is set to be zero. This adatom exchange coefficient becomes terrace width independent[29] when the rate-limiting process is adatom attachment/detachment at the step ($\Gamma_\pm w \ll D_s c_0 \Omega^2$) and we then have

$$\partial_t x_n = \frac{\Gamma_+ \Gamma_-}{\Omega k_B T (\Gamma_+ + \Gamma_-)} [2\mu_n - \mu_{n+1} - \mu_{n-1}]. \tag{13}$$

In the opposite diffusion limited case ($\Gamma_\pm w \gg D_s c_0 \Omega^2$) Eq. (11) becomes

$$\partial_t x_n = \frac{\Omega D_s c_0}{k_B T} \left[\frac{\mu_n - \mu_{n-1}}{w_{n-1}} + \frac{\mu_n - \mu_{n+1}}{w_n} \right], \tag{14}$$

as suggested by Rettori and Villain.[27]

Now let us consider the motion of a fluctuating step in a 2D step array. The step velocity in this general case can be written as

$$\partial_t x_n = \sum_{n'=1}^{N_s} \int_0^{L_y} dy' D(x_n(y);x_{n'}(y'))[\mu_n(y)-\mu_{n'}(y')], \tag{15}$$

assuming first-order kinetics with an adatom exchange coefficient matrix, $D(x_n(y);x_{n'}(y'))$ between two points on the steps. In principle, to test the validity of the above equation and to find the matrix element, $D(x_n(y);x_{n'}(y'))$, one should solve the adatom diffusion equation on a terrace with boundary conditions at the fluctuating steps. However, such a solution is extremely difficult in general. Here, we discuss some limits that may yield good approximations in some experimentally relevant cases.

First, let us consider the case of *global* mass movement, in which adatom exchange between any two points on steps occurs through a global (constant chemical potential) reservoir. In this case, the adatom exchange coefficient is constant, $D(x_n(y);x_{n'}(y'))=\Gamma_A/(\Omega N_s L_y k_B T)$, and the step velocity of Eq. (15) becomes

$$\begin{aligned}\partial_t x_n &= \frac{\Gamma_A}{\Omega k_B T}\left[\mu_n(y) - \frac{1}{N_s L_y}\sum_{n'=1}^{N_s}\int_0^{L_y} dy' \mu_{n'}(y')\right] \\ &= \frac{\Gamma_A}{\Omega k_B T}[\mu_n(y)-\mu_{\rm res}],\end{aligned} \tag{16}$$

where the reservoir chemical potential is given as the overall average step chemical potential, $\mu_{\rm res}=(1/N_sL_y)\Sigma_{n=1}^{N_s}\int_0^{L_y}dy\,\mu_n(y)$. This is identically zero when the step chemical potential of Eq. (5) is used. This effective global adatom exchange mechanism is physically relevant when the attachment/detachment rate at steps is very slow compared to the surface diffusion and adatom hopping rates, so that the adatom can freely diffuse to any place on the surface in a typical attachment/detachment interval.

If the attachment/detachment at the step is the rate-limiting process but there are no direct adatom hops between different terraces, then locally conserved kinetics should be used[29] and the motions of neighboring steps are coupled together. In this case, rapid diffusion on a terrace ensures that each terrace has a spatially uniform adatom chemical potential, though its value is not the same, in general, on different terraces. Using the quasistatic approximation, the chemical potential on the nth terrace, μ_n^t, can be obtained from adatom conservation on the terrace,[29]

$$\mu_n^t = (\Gamma_+\overline{\mu_n}+\Gamma_-\overline{\mu_{n+1}})/(\Gamma_++\Gamma_-), \tag{17}$$

where $\overline{\mu_n}=(1/L_y)\int_0^{L_y}dy\,\mu_n(y)$ is the average nth step chemical potential. Since steps move according to the chemical potential difference between the step and the terrace, the step velocity is given by

$$\begin{aligned}\partial_t x_n(y) &= \frac{\Gamma_+}{\Omega k_B T}[\mu_n(y)-\mu_n^t]+\frac{\Gamma_-}{\Omega k_B T}[\mu_n(y)-\mu_{n-1}^t] \\ &= \frac{\Gamma_+^2+\Gamma_-^2}{\Omega k_B T(\Gamma_++\Gamma_-)}[\mu_n(y)-\overline{\mu_n}] \\ &\quad + \frac{\Gamma_+\Gamma_-}{\Omega k_B T(\Gamma_++\Gamma_-)}[2\mu_n(y)-\overline{\mu_{n+1}}-\overline{\mu_{n-1}}]\end{aligned} \tag{18}$$

and reduces to the velocity of the quasi-1D case with the fast diffusion case [Eq. (13)] in the 1D limit of $\mu_n(y)=\overline{\mu_n}$.

Since L_y is much larger than the terrace width w in a typical vicinal surface system, it is conceivable that the adatoms on the terrace may not diffuse along the step direction all the way to the end of the system in a typical attachment/detachment time interval, even when it is much slower than the diffusion time to the neighboring step across the terrace, i.e., when $D_s c_0\Omega^2/w \gg \Gamma_\pm > D_s c_0\Omega^2/L_y$. In this case, the local chemical potential on the terrace should be obtained by averaging the step chemical potential over the diffusion distance l_d in the y direction and will show a weak y dependence. Therefore, Eq. (17) should be replaced by

$$\mu_n^t(y) = \frac{\Gamma_-}{\Gamma_++\Gamma_-}\overline{\mu_n^-}(y)+\frac{\Gamma_+}{\Gamma_++\Gamma_-}\overline{\mu_{n+1}^+}(y), \tag{19}$$

with

$$\overline{\mu_n^\pm}(y) = \int_0^{L_y}\mu_n(y')K(l_d^\pm;y-y')dy', \tag{20}$$

where the normalized smearing kernel $K(l_d^\pm;r)$ has the cutoff distance $l_d^\pm = D_s c_0\Omega^2/\Gamma_\pm$ [for example, $K(l_d;r)\sim e^{-|r|/l_d}$].

If the surface diffusion is slow enough (or the attachment/detachment rate is fast enough) that the diffusion length on the terrace during a typical attachment/detachment interval becomes of order w or less, i.e., $D_s c_0\Omega^2/w \leqslant \Gamma_\pm$, then the adatom exchange rate becomes a function of the distance between two points. To obtain a step velocity, we should in principle include mass transport modes between two points with different y positions on the steps. However, for the step bunching or unbunching dynamics in which steps remain nearly straight, the variation of step chemical potential in the y direction is much smaller than in the x direction and can be ignored. Thus we approximate the step velocity by

$$\begin{aligned}\partial_t x_n(y) &= \frac{\Gamma_e(w_n(y))}{\Omega k_B T}[\mu_n(y)-\mu_{n+1}(y)] \\ &\quad + \frac{\Gamma_e(w_{n-1}(y))}{\Omega k_B T}[\mu_n(y)-\mu_{n-1}(y)],\end{aligned} \tag{21}$$

with the effective adatom exchange coefficient of Eq. (12).

III. NUMERICAL CALCULATIONS AND RESULTS

We consider faceting in the nucleation regime where the critical width w_c is larger than the average step spacing w_a

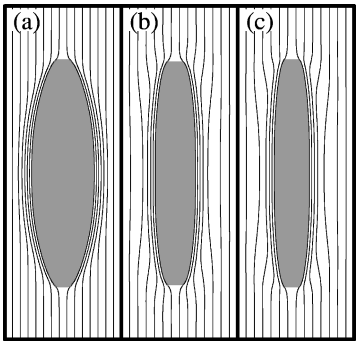

FIG. 2. Top view of step configurations near a growing nucleus with global mass transport in case A (a) and local mass transport in case B (b) and case C (c). In all cases, $w_c/w_a=1.8$ and $w_b/w_a=1/4$ with $w_a=10$ in atomic units. The reconstruction energy ϵ_R, line tension $\tilde{\beta}$, and the kinetic parameter Γ are adopted from Ref. 21; $\epsilon_R=0.006$, $\Gamma_s=1.5\times10^4$ sec^{-1}, and $\tilde{\beta}=100$ in units of atomic size and thermal energy k_BT. Each panel shows a 160×3000 size configuration. The starting seed nuclei sizes are the same (25×70). The configurations shown are when the lateral size of the reconstructed region is around 2000, which is obtained at $t=7.5\times10^{-3}$ sec for (a), at $t=7.6\times10^{-3}$ sec for (b), and at $t=4.4\times10^{-2}$ sec for (c).

(say $w_c\approx2w_a$). Initially we create a nucleus of reconstructed terrace by hand and first calculate the deterministic time evolution of its growth.

For the reconstruction dynamics, we use Eq. (9), while for step dynamics we consider three limiting mass transport cases: global mass movement (case A) of Eq. (16), local mass movement with attachment/detachment rate-limiting kinetics (case B) of Eq. (18), and the diffusion rate-limiting case (case C) of Eq. (21). The possible effect of a Schwoebel barrier[30] is not considered, i.e., we always set $\Gamma_+=\Gamma_-=\Gamma$. The kinetic parameter Γ and the reconstruction energy parameter ϵ_R and ϵ_s are adopted from Liu *et al.* for the Si(111) surface.[21] For the step dynamics with global mass exchange, case A, we assume that a global reservoir is formed on the terrace and set $\Gamma_A=2\Gamma$. For case B $(D_sc_0\Omega^2/w\gg\Gamma_\pm)$, we consider the case when the length of each terrace, L_y, is much larger than the diffusion length, $l_d^\pm=D_sc_0\Omega^2$ and use Eq. (19) to calculate the terrace chemical potential. We choose $l_d/w_a=20$ while L_y/w_a is typically chosen to be around 500. For case C, we choose $D_sc_0\Omega^2=\Gamma w_a$ such that the diffusion time across the terrace (with width w_a) is of the order of a typical attachment/detachment interval.

Figure 2 shows typical step configurations in the early stage of the faceting in all three cases. In case A, with nonlocal mass transport, as the reconstructed facet grows it causes neighboring terraces to become *smaller*. There is a smooth relaxation to the average width far from the facet. Step spacings in cases B and C, with local mass transport, show more interesting behavior because of the correlated step motion. While a region of step bunching is again observed close to the facet, on the other side of the bunch there are also some terraces that are *wider* than average. As the facet continues to grow, the number of steps in the bunched region increases but the widths of the wider terraces in front of the step bunch also increase. One of these may become sufficiently wide to serve as new nucleus for reconstruction.

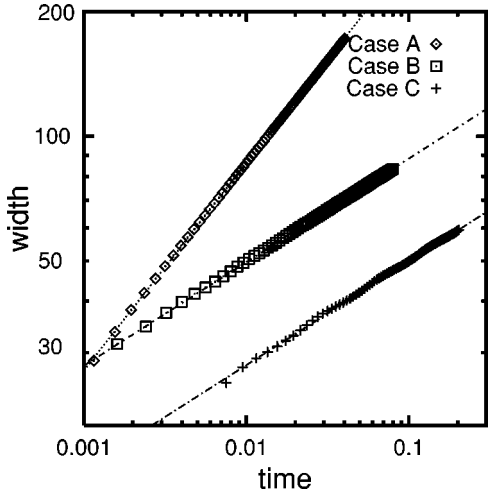

FIG. 3. Measured time dependences of the facet widths for three cases are shown in a log-log plot. All data in each case fall on a line indicating that the reconstructed terrace width increases as $w\sim at^\alpha$. The α values of the fitting lines are 1/2 for case A and 1/4 for cases B and C.

This *induced nucleation process*[7] can repeat itself many times, producing a rather regular pattern of faceted and bunched regions that may be relevant for experiment.[31,32] We will discuss this mechanism in more detail later.

A. Isolated facet growth

Before doing this, let us first consider the growth rate of an *isolated* facet. We artificially prevent the formation of other (induced) nuclei on all other terraces by setting R_n to zero except on the terrace on which the original nucleation occurred. We then measure the time dependence of the facet length and width during growth. We adopted parameters from Ref. 21 and chose $\epsilon_R=0.006$, $\tilde{\beta}=100$, and $\Gamma=1.5\times10^4$ sec^{-1} where the atomic size and thermal energy k_BT are set to unity. We assume fast dynamics for reconstruction and set the response for the reconstruction to be fifty times faster than step motion. ($\Gamma_R=50\Gamma$ when they are represented in terms of dimensionless quantities.) In all three cases shown in Fig. 2, the average terrace width is $w_a=10$. ϵ_s and g are chosen such that the critical width $w_c=\epsilon_s/\epsilon_R$ and the terrace width in the step bunch $w_b=(2g/e_R)^{1/3}$ (Ref. 7) will be $1.8w_a$ and $(1/4)w_a$, respectively. In all cases the reconstructed region propagates in the y direction with a *constant* velocity (after an initial transient where it forms the elongated shape) of $v_y=2.7\times10^5$ sec^{-1} for case A, $v_y=2.6\times10^5$ sec^{-1} for case B, and $v_y=4.5\times10^4$ sec^{-1} for case C. Linear growth along the step direction has been seen in experiment[2] and there are general theoretical arguments for constant facet tip velocity.[21]

On the other hand, the growth rate of the *normal* width of the case A (without local conservation) is different from that of cases B or C (with local conservation). Figure 3 shows the growth of the facet width versus time in a log-log plot. All data in each case fall into a straight line, indicating that the reconstructed terrace width increases as $w\sim at^\alpha$. In case A, the facet grows as $t^{1/2}$, while it grows as $t^{1/4}$ for cases B and C. These results agree with the predictions of the classic 1D

continuum model of Mullins.[33] Note that the surface configurations of case *C* in Fig. 2 are similar to those of case *B* when two configurations with the same lateral size are compared, though it takes much longer to grow to the same lateral size in case *C*. It takes the same order of magnitude of time for cases *A* and *B* to form the reconstruction shown in the figure while it takes around 6 times longer for case *C*.

B. Induced nucleation

Let us now relax the constraint forbidding other nuclei from forming. Even if thermal fluctuations were included, this should produce essentially no change in case *A*. Since all terraces near the original facet become smaller on average, other thermally nucleated facets are *less* likely to occur nearby.

The story is quite different in cases *B* and *C* with local mass transport, where *induced* nuclei can form and inhibit the further growth of the original facet. In these cases, the motion of a step is directly coupled to the motion of neighboring steps. Initially, as the step bounding the reconstructed terrace moves forward to increase the reconstructed terrace's width, the neighboring step must move backward to conserve adatoms locally. Thus both the original reconstructed terrace and the terrace in front of the step that moves backward get wider. When the two steps that move in opposite directions come sufficiently close to each other for step repulsions to become important (with spacing approaching that of the equilibrium step bunch), they ''collide'' and both begin to move forward together as a bunch because of the driving force from the reconstructed terrace behind. Then the local conservation process repeats itself, causing new steps in front of the advancing step bunch to move backward and making the terraces in front of those steps wider. As the original facet grows, the number of steps in the bunch increases and the widths of the widest terraces in front of the step bunch also increase. Such sufficiently wide terraces can be nuclei for the reconstruction of another facet.

A quantitative treatment of this induced nucleation mechanism using a 1D model was carried out by the authors.[7] When the typical distance between steps in a step bunch $w_b \sim (2g/\epsilon_r)^{1/3}$ is much smaller than the average terrace width w_a, it was shown that only one other terrace, aside from the original facet, is larger than w_a at any given time. In the limit that w_b/w_a goes to zero, the maximum width of the induced wide terrace increases *linearly* with the number of steps n_b in the bunch, separating it from the original facet. Moreover it remains as the widest terrace for an increasing long time interval, $\Delta t \sim n_b^3$. Once it gets larger than w_c, reconstruction will occur. Further growth of the original facet essentially stops, but the new facet can induce another nucleus on the other side as it continues to grow. Then this new nucleus can induce another one and so on. The velocity of the nucleation front is *linear* in time because it always takes the same amount of time to induce a nucleus. Hence the faceted surfaces arising from this idealized process have a periodic distribution of reconstructed terraces separated by step bunches.

Figure 4 illustrates the propagation of nucleation through the induced nucleation mechanism in case *C* as given by the present 2D model. (A similar result is expected for case *B* since the surface configurations of case *B* in Fig. 2 are similar to those of the case *C* except for the time scale.) The left panels are the top views of step configurations at three different times in the deterministic case while the right panels are those with thermal noise. (The effects of thermal noise are discussed in Sec. III C.) A nucleus of reconstructed terrace is created by hand at the middle terrace. From the upper panel, one can see that some terraces in front of the step bunch become wider as mentioned. As time goes on, the widths of the wider terraces increase and, at some point, one of the wider terraces becomes wide enough to become a new nucleus as shown in the middle panel. As this nucleus grows, it induces another nucleus (lower panel) and the process repeats itself.

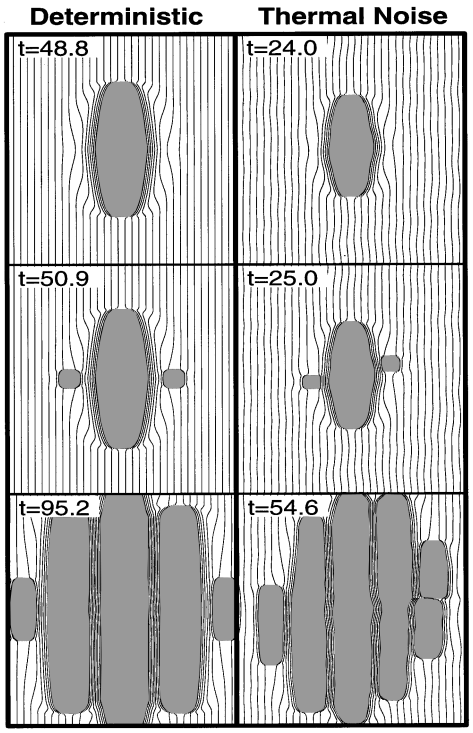

FIG. 4. Propagation of nuclei through induced nucleation. Step configurations at three different times are shown for both deterministic (left panels) and Langevin (right panels) dynamics. The times shown are in units of milliseconds from the creation of the initial nucleus. Left panel sizes are 320×12800 in atomic units and the right ones are 320×8000. The same parameters as in Fig. 2 are used.

A few remarks should be made on the difference in growth of an induced facet and the initial isolated facet. First, the propagation in the *y* direction of an induced nucleus is initially faster than the original isolated one since mass conservation induces an elongated wider terrace region even before the reconstruction on the region takes place. Second, an induced facet grows essentially only on one side in the *x* direction while the original one grows on both sides. This asymmetric propagation, together with the faster initial *y*-direction growth, cause the induced nuclei to grow more rapidly. However, as discussed below, these differences are not as noticeable when thermal noise is taken into account.

C. Effects of thermal noise on induced nucleation

When thermal fluctuations are considered, these regular patterns, selected by a kinetic mechanism, would be ex-

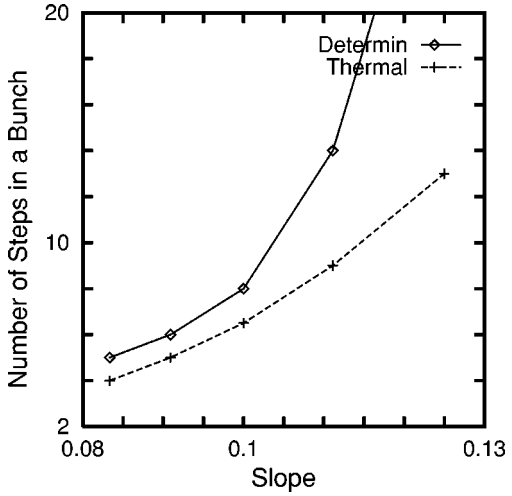

FIG. 5. Number of steps in a step bunch vs the slope of the vicinal surface with (cross) and without (open diamond) noise. As in the previous figures we choose the parameter set $w_c=18$, $w_b=2.5$. The number of steps in a bunch are numerically calculated for different values of w_a.

pected to be less sharp. Particularly when w_b/w_a is not so small, the effects of mass conservation are spread out over many terraces and several terraces in front of the step bunch become larger than w_a. Since there are then many large terraces on which thermal nucleation could occur, nucleation sites and times are less precisely determined in this case. However, in general, the number of steps n_b in a bunch when induced nucleation takes place is expected to be smaller than the value predicted by the 1D model or the deterministic case.

With the parameters given in Fig. 2 but with a smaller w_a, for example, $w_a=8$, it may take very long to create an induced wide terrace with width greater than w_c. However, in the presence of noise, step fluctuations leading to a nucleus can happen on terraces whose averaged width is *smaller* than w_c. The required time for this thermally assisted nucleation decreases rapidly with increasing average terrace width. As the number of steps in a bunch n_b increases, the average width of terraces in the induced wide terrace region also increases, and hence the nucleation times on these terraces decrease. Moreover, the time interval Δt in which the terrace in front of the step bunch remains as the widest one before it joins the step bunch, increases with n_b. Therefore, as bunching proceeds, there will be a bunch size n_b such that $\Delta t(n_b)$ becomes larger than the nucleation time, leading to the formation of an induced nucleus. In general this bunch size will be smaller than the critical bunch size predicted by the 1D model. Since both Δt and the nucleation time vary rapidly with the number of steps in the bunch, faceted surfaces produced under conditions of local mass conservation may show rather strong regularities even when the nuclei are created in part by thermal step fluctuations.

The final periodicity dependence on the slope of the vicinal surface is shown in Fig. 5. The predicted number of steps in a step bunch, both in the deterministic case and the case with thermal fluctuations, are numerically calculated for five different values of w_a, with the same w_c and w_b. For the case with thermal fluctuations (open diamond), step-bunch sizes are obtained by averaging the results of five independent runs. The noise strengths are given by the fluctuation-dissipation theorem; we used conserved noise for the step fluctuations and nonconserved noise for the reconstruction. As expected, the periodicities are always smaller and less sensitive to change of the average slope of the vicinal surface when we consider thermal fluctuations. In future work we plan to study the dependence of the expected final periodicity on other parameters and under more general conditions. A particularly interesting case arises when induced nucleation, a dynamical process, cooperates with some energetic effect, like a surface-stress-induced elastic energy, which also could favor periodic structures.[34]

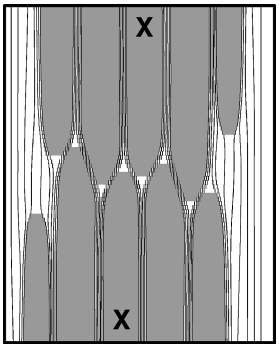

FIG. 6. Top view of step configurations in case *B* arising from interaction between two nuclei through an induced nucleation mechanism is shown. The initial positions of the nuclei (created by hand) are on the terraces marked by *X* but outside the figure.

D. 2D patterns from induced nucleation

An interesting 2D pattern arises from induced nucleation using Eq. (21) when two (thermal) nuclei form that are close in the x direction but separated by a large distance in the y direction. Figure 6 shows a step configuration in case *C* in the deterministic limit arising from two such nuclei (created by hand on the terraces marked by X). As time goes on, each nucleus grows as $t^{1/4}$ in the normal direction until it produces its own induced nucleus. In the lateral direction, nuclei grow essentially linearly in t until they ''collide'' with each other and trap a bunch of *crossing steps* between them. After such an encounter, the growth of the nuclei in the y direction essentially stops. The number of steps in the crossing step bunch is determined by how many steps initially separated the two nuclei when they formed. Once this configuration forms, induced nuclei from the two original facets will produce new crossing steps at essentially the same y position as the original crossing steps. Hence, an *alignment* of crossing step bunches is formed as shown in Fig. 6. The number of steps in the induced crossing bunches are expected to be the same as that in the original crossing step bunch when the idealized induced nucleation mechanism of the 1D model is accurate.

A strong tendency for alignment of crossing steps has been found in some step bunching experiments on vicinal GaAs(001).[3] At present it is not clear whether this is a purely kinetic phenomenon as our model would suggest, or an equilibrium phenomenon from some energetic (probably elastic) effect, though the strong regularity favors the latter hypothesis. It is also possible that these patterns of regular step

bunches can be formed on the surfaces of real materials through the cooperation of the two effects.

IV. CONCLUSION

In summary, we have studied a 2D model of coupled step motion and reconstruction for reconstruction-driven faceting in the nucleation regime. An isolated nucleated facet grows linearly with time in the step direction. Its width grows as $t^{1/2}$ when the mass movement is global. With local mass flow, the facet width grows as $t^{1/4}$ asymptotically, as the previously studied 1D models predicted.

When the mass transport is local, the motions of neighboring steps are directly coupled in such a way that a growing nucleus can induce the formation of another nucleus nearby. This can create a propagation of nucleation events leading to regular arrangements of reconstructed facets separated by step bunches. When thermal fluctuations are taken into account, this induced nucleation mechanism will produce less sharp regularities in the faceted surface. Nevertheless, when thermal fluctuations are incorporated into the induced nucleation model, the qualitative features of the induced nucleation mechanism as discussed here remain valid and are expected to be observed under more robust conditions than the deterministic models would predict. While there are a number of different factors (including in particular elastic interactions[5,6]) that can contribute to the facet spacing in particular systems, induced nucleation represents a very general *kinetic* mechanism that should be considered in analyzing experimental data.

ACKNOWLEDGMENTS

We are grateful to D.-J. Liu, J. Reutt-Robey, and E. D. Williams for helpful discussions. This work was supported by NSF-MRSEC Grant No. DMR96-3252.

APPENDIX: DERIVATION OF THE EFFECTIVE ADATOM EXCHANGE COEFFICIENT BETWEEN STEPS [EQ. (12)]

Equation (12) can be easily derived from an analogy with the conductance in a series electrical circuit. The changes in step velocity due to adatom exchange between two steps are *linearly proportional* to the adatom *current* between the two steps. Hence the effective adatom exchange coefficient given by Eq. (12) is inversely proportional to the effective ''resistance'' R_e between the two steps, defined by $R_e=\Delta\mu/j$, where j is the current and $\Delta\mu$ is the step chemical potential difference. When an atom moves from one step to the neighboring step, it goes through three processes: a detachment from the step, surface diffusion on the terrace, and an attachment to the other step. In other words, during an exchange of an atom between two neighboring steps, it passes through three resistors in series: R_t associated with surface diffusion and R_+ and R_- associated with attachment/detachment at the left and the right steps. This analogy with a series electric circuit becomes exact in the quasistatic approximation, where the step motions are much slower than the adatom movements. Then mass conservation guarantees that the currents through the three ''resistors'' are the same.

Here, we calculate $R_\pm$ and R_t in terms of the usual kinetic parameters, step mobility $\Gamma_\pm$, and surface diffusion constant D_s and obtain Γ_e by calculating the current j in the quasistatic approximation. Without loss of generality, let us assume ascending steps and denote the step chemical potentials at the left and the right steps as μ_s^- and μ_s^+. Let $\mu_t(x)$ be the chemical potential on the terrace and μ_t^- and μ_t^+ be the terrace chemical potential at the boundaries, i.e., $\mu_t^\pm=\lim_{x\to x_\pm}\mu_t(x)$ where x_- $[x_+]$ is the position of the left (right) step. When we assume small excess adatom concentration, $\delta c(x)=c(x)-c_0\ll c_0$ on the terrace such that $\delta c(x)=c_0(e^{\mu_t(x)/k_BT}-1)\approx(c_0/k_BT)\mu_t(x)$, the current on the terrace, j_t is proportional to $(\mu_t^- - \mu_t^+)$:

$$j_t=-D_s\partial_x c\approx-\frac{D_s c_0}{k_BT}\partial_x\mu_t=\frac{D_s c_0}{k_BTw}(\mu_t^- - \mu_t^+). \quad \text{(A1)}$$

In the last step, we used the linearity of the terrace chemical potential profile $\partial_x\mu_t=(\mu_t^- - \mu_t^+)/w$, which came from $\partial_x^2 c(x)=0$ with $\mu_t(x)\sim c(x)$. From Eq. (A1), we see that the terrace resistance $R_t\equiv(\mu_t^- - \mu_t^+)/j_t$ is given by

$$R_t=k_BTw/D_s c_0. \quad \text{(A2)}$$

On the other hand, at the boundaries, adatom currents $j_\pm=\pm\partial_t x_\pm/\Omega$ are given by

$$j_\pm=\mp\frac{\Gamma_\mp}{\Omega^2 k_BT}(\mu_s^\pm-\mu_t^\pm) \quad \text{(A3)}$$

and the resistances at the steps $R_\pm\equiv\mp(\mu_s^\pm-\mu_t^\pm)/j_\pm$ are, therefore, given by

$$R_\pm=\Omega^2 k_BT/\Gamma_\mp. \quad \text{(A4)}$$

To obtain the total effective exchange coefficient Γ_e, defined by

$$j\equiv\frac{\Gamma_e}{\Omega^2 k_BT}(\mu_s^- - \mu_s^+), \quad \text{(A5)}$$

we need to calculate the current across the two steps, j. This can be easily done in the quasistatic approximation where three currents of Eqs. (A1) and (A3) should be the same. This requirement fixes $\mu_t^\pm$:

$$\mu_t^\pm=\mu_s^\pm\pm R_\pm j \quad \text{(A6)}$$

with $j=(\mu_s^- - \mu_s^+)/(R_+ + R_t + R_-)$ as expected from the analogy with a series circuit and we have

$$\Gamma_e=[\Omega^2 k_BT(R_+ + R_t + R_-)]^{-1}$$
$$=\left[\frac{1}{\Gamma_+}+\frac{w}{D_s c_0\Omega^2}+\frac{1}{\Gamma_-}\right]^{-1}. \quad \text{(A7)}$$

[1] E. D. Williams and N. C. Bartelt, in *Handbook of Surface Science*, edited by W. N. Unertl (North-Holland, Amsterdam, 1996), pp. 51–99.
[2] R. J. Phaneuf, N. C. Bartelt, E. D. Williams, W. Święch, and E. Bauer, Phys. Rev. Lett. **67**, 2986 (1991).
[3] K. Hata *et al.*, Appl. Phys. Lett. **76**, 5601 (1994).
[4] J. Ozcomert, W. Pai, N. Bartelt, and J. Reutt-Robey, Phys. Rev. Lett. **72**, 258 (1994).
[5] M. Yoon, S. G. J. Mochrie, D. M. Zehner, G. M. Watson, and D. Gibbs, Surf. Sci. **338**, 225 (1995).
[6] F. Pourmir, S. Rousset, S. Gauthier, M. Sotto, J. Klein, and J. Lecoeur, Surf. Sci. **324**, L337 (1995).
[7] H.-C. Jeong and J. D. Weeks, Phys. Rev. Lett. **75**, 4456 (1995).
[8] J. D. Weeks, D.-J. Liu, and H.-C. Jeong, in *Dynamics of Crystal Surfaces and Interfaces*, edited by P. Duxbury and T. Pence (Plenum Press, New York, 1997), p. 199.
[9] E. D. Williams and H.-C. Jeong (unpublished).
[10] G. Bilalbegović, F. Eroclessi, and E. Tosatti, Europhys. Lett. **18**, 163 (1992).
[11] K. G. Wilson, Rev. Mod. Phys. **47**, 773 (1975).
[12] S. T. Chui and J. D. Weeks, Phys. Rev. B **14**, 4978 (1976).
[13] F. Katsuki and K. Kamei, Appl. Surf. Sci. **94/95**, 485 (1996).
[14] T. Niemeijer and J. van Leeuwen, in *Phase Transitions and Critical Phenomena*, edited by C. Domb and M. Green (Academic Press, London, 1976), Vol. 6, p. 425.
[15] R. Evans, in *Fundamentals of Inhomogeneous Fluids*, edited by D. Henderson (Dekker, New York, 1992).
[16] D.-J. Liu and J. D. Weeks, Phys. Rev. Lett. **79**, 1694 (1997).
[17] D. B. Abraham, Phys. Rev. Lett. **51**, 1279 (1983).
[18] M. P. A. Fisher, D. S. Fisher, and J. D. Weeks, Phys. Rev. Lett. **48**, 368 (1982).
[19] E. E. Gruber and W. W. Mullins, J. Phys. Chem. Solids **28**, 875 (1967).
[20] C. Jayaprakash, C. Rottman, and W. F. Saam, Phys. Rev. B **30**, 6549 (1984).
[21] D.-J. Liu, J. D. Weeks, M. D. Johnson, and E. D. Williams, Phys. Rev. B **55**, 7653 (1997).
[22] Note that the short-wavelength fluctuations of the steps, which are responsible for much of the entropic repulsion, are not considered explicitly in this approach. We assume that these short-wavelength fluctuations give rise to effective interactions between smoothed steps like those in the 1D model after coarse graining.
[23] R. J. Phaneuf, N. C. Bartelt, E. D. Williams, W. Święch, and E. Bauer, Phys. Rev. Lett. **71**, 2284 (1993).
[24] We could use a $g(R)$ that interpolates between two different g values for reconstructed and unreconstructed surfaces but the effect of R dependence of g is very small for faceting through nucleation since the reconstructed terraces are much wider than the other terraces and for these $g(R)/w^3$ is negligible. Hence we do not consider the R dependence of g. Similarly, we do not consider the R dependence of $\tilde{\beta}$ in Eq. (2).
[25] P. Nozières, J. Phys. (France) **48**, 1605 (1987).
[26] N. C. Bartelt, T. L. Einstein, and E. D. Williams, Surf. Sci. **276**, 308 (1992).
[27] A. Rettori and J. Villain, J. Phys. (France) **49**, 257 (1988).
[28] M. Ozdemir and A. Zangwill, Phys. Rev. B **42**, 5013 (1990).
[29] D.-J. Liu, E. S. Fu, M. D. Johnson, J. D. Weeks, and E. Williams, J. Vac. Sci. Technol. B **14**, 2799 (1996).
[30] R. L. Schwoebel and E. J. Shipsey, J. Appl. Phys. **37**, 3682 (1966).
[31] H. Hibino, Y. Homma, and T. Ogino, Phys. Rev. B **51**, 7753 (1995).
[32] J. R. Heffelfinger, M. W. Bench, and C. B. Carter, Surf. Sci. **343**, L1161 (1995).
[33] W. W. Mullins, J. Appl. Phys. **28**, 333 (1957).
[34] S. Song, S. G. J. Mochrie, and G. B. Stephenson, Phys. Rev. Lett. **74**, 5240 (1995).